QCD Factorization in B Decays into $\rho\pi$

X.-H. Guo[†1], O.M.A. Leitner[†,‡2], A.W. Thomas[†3]

[†] *Department of Physics and*
Special Research Centre for the Subatomic Structure of Matter,
University of Adelaide, Adelaide 5005, Australia
[‡] *Laboratoire de Physique Corpusculaire de Clermont-Ferrand*
IN2P3/CNRS Université Blaise Pascal
F-63177 Aubière Cedex France

Abstract. Based on the QCD factorization approach we analyse the branching ratios for the channel $B \to \rho\pi$. From the comparisons with experimental data provided by CLEO, BELLE and BABAR we constrain the form factor $F^{B\to\pi}(m_\rho^2)$ and propose boundaries for this form factor depending on the CKM matrix element parameters ρ and η.

1. NAIVE FACTORIZATION

The investigation of B decays requires a knowledge of both the soft and hard interactions which control the dynamics of quarks and gluons. Because the energy involved in B decays covers a large range, from m_b down to Λ_{QCD}, it is necessary to describe the phenomenon with accuracy. Recently, the BELLE, BABAR, and CLEO facilities have been providing more and more data which can be compared with theoretical results and hence increase our knowledge in this area.

In any phenomenological treatment of the weak decays of hadrons, the starting point is the weak effective Hamiltonian at low energy [1, 2, 3, 4, 5]. It is obtained by integrating out the heavy fields (e.g. the top quark, W and Z bosons) from the Standard Model Lagrangian. It can be written as,

$$\mathscr{H}_{eff} = \frac{G_F}{\sqrt{2}} \sum_i V_{CKM} C_i(\mu) O_i(\mu) \ , \tag{1}$$

where G_F is the Fermi constant, V_{CKM} is the CKM matrix element, $C_i(\mu)$ are the Wilson coefficients, $O_i(\mu)$ are the operators entering the Operator Product Expansion and μ represents the renormalization scale. In the present case, since we analyse direct CP violation in B decays into $\rho\pi$, we take into account both tree and penguin operators and

[1] xhguo@physics.adelaide.edu.au
[2] oleitner@physics.adelaide.edu.au
[3] athomas@physics.adelaide.edu.au

CP689, *Neutrinos, Flavor Physics, and Precision Cosmology:*
Fourth Tropical Workshop on Particle Physics and Cosmology, edited by J. F. Nieves and R. R. Volkas

the effective Hamiltonian is,

$$\mathscr{H}_{eff}^{\triangle B=1} = \frac{G_F}{\sqrt{2}}\left[V_{ub}V_{uq}^{*}\left(C_1O_1^q + C_2O_2^q\right) - V_{tb}V_{tq}^{*}\sum_{i=3}^{10}C_iO_i\right] + h.c.\ , \tag{2}$$

where $q = d$. Consequently, the decay amplitude can be expressed as follows,

$$A(B \to PV) = \frac{G_F}{\sqrt{2}}\left[V_{ub}V_{uq}^{*}\left(C_1\langle PV|O_1^q|B\rangle + C_2\langle PV|O_2^q|B\rangle\right) - V_{tb}V_{tq}^{*}\sum_{i=3}^{10}C_i\langle PV|O_i|B\rangle\right] + h.c.\ , \tag{3}$$

where $\langle PV|O_i|B\rangle$ are the hadronic matrix elements, and $P(V)$ indicates a pseudoscalar (vector) meson. The matrix elements describe the transition between initial and final state at scales lower than μ and include, up to now, the main uncertainties in the calculation because it involves the non-perturbative physics.

The computation of the hadronic matrix elements, $\langle PV|O_i|B\rangle$, is not trivial and requires some assumptions. The general method which has been used is the so-called "factorization" procedure [6, 7, 8], in which one approximates the matrix element as a product of a transition matrix element between a B meson and one final state meson and a matrix element which describes the creation of the second meson from the vacuum. This can be formulated as,

$$\begin{aligned} \langle PV|O_i|B\rangle &= \langle V|J_{2i}|0\rangle\ \langle P|J_{1i}|B\rangle\ , \\ \text{or}\ \ \langle PV|O_i|B\rangle &= \langle P|J_{4i}|0\rangle\ \langle V|J_{3i}|B\rangle\ , \end{aligned} \tag{4}$$

where the J_{ji} are the transition currents. This approach is known as *naive* factorization since it factorizes $\langle PV|O_i|B\rangle$ into a simple product of two quark matrix elements, (see Fig. 1). Analytically, Fig. 1 can be written down as,

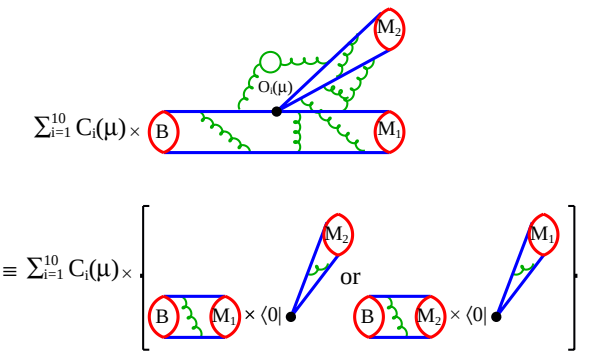

FIGURE 1. Naive factorization, where M_1 and M_2 represent the final meson states.

$$A(B \to PV) \propto \left[\sum_{i=1}^{10} V_{CKM} C_i(\mu) \langle M_1 M_2 | O_i | B \rangle \right]$$
$$\propto \left[\sum_{i=1}^{10} V_{CKM} C_i(\mu) \langle M_1 | J_{2i} | 0 \rangle \langle M_2 | J_{1i} | B \rangle \right] . \quad (5)$$

A possible justification for this approximation has been given by Bjorken [9]: the heavy quark decays are very energetic, so the quark-antiquark pair in a meson in the final state moves very fast away from the localised weak interaction. The hadronization of the quark-antiquark pair occurs far away from the remaining quarks. Then, the meson can be factorized out and the interaction between the quark pair in the meson and the remaining quark is tiny.

The main uncertainty in this approach is that the final state interactions (FSI) are neglected. Corrections associated with the factorization hypothesis are parameterized [10, 11, 12] and hence there maybe large uncertainties [13]. In spite of this, there are indications that should give a good estimate of the magnitude of the B decay amplitude in many cases [14, 15]. In order to improve the estimate of the hadronic matrix element, we will briefly present in Section 2 the formalism of QCD factorization, which is an extension of naive factorization. We will see how it is possible to incorporate QCD corrections in order to include the FSI at the first order in α_s into the factorization approach. In Section 3, we will list our numerical results for the branching ratios related to the channels $B \to \rho\pi$ and $B \to \omega\pi$. In Section 4, we will constrain the form factor $F_1^{B\to\pi}$ and propose boundaries for this form factor depending on the CKM matrix element parameters ρ and η. Finally, in the last section we will summarize our analysis and draw some conclusions.

2. QCD FACTORIZATION

Factorization in charmless B decays involves three fundamental scales: the weak interaction scale M_W, the b quark mass scale m_b, and the strong interaction scale Λ_{QCD}. It is well known that the non-leptonic decay amplitude for $B \to PV$ is proportional to:

$$A(B \to PV) \propto \sum_i C_i(\mu) \langle PV | O_i(\mu) | B \rangle , \quad (6)$$

where we have omitted the CKM factor and Fermi constant for simplicity. The matrix elements $\langle PV|O_i(\mu)|B\rangle$ contain non-perturbative effects which cannot be accurately evaluated. The coefficients $C_i(\mu)$ include strong interaction effects from the scales M_W down to m_b and is under control. The aim is therefore to obtain a good estimate of the matrix elements without assuming naive factorization. In QCD factorization (QCDF), assuming a heavy quark expansion when $m_b \gg \Lambda_{QCD}$ and soft collinear factorization where the particle energies are bigger than the scale Λ_{QCD}, the matrix elements $\langle PV|O_i(\mu)|B\rangle$ can be written as [16]:

$$\langle PV | O_i(\mu) | B \rangle = \langle P | j_1 | B \rangle \langle V | j_2 | 0 \rangle \left[1 + \sum_n r_n \alpha_s^n + \mathcal{O}(\Lambda_{QCD}/m_b) \right] , \quad (7)$$

where r_n refers to the radiative corrections in α_s and j_i are the quark currents. It is straightforward to see that if we neglect the corrections at the order α_s, we recover the conventional naive factorization in the heavy quark limit. We can rewrite the matrix elements $\langle PV|O_i(\mu)|B\rangle$, at the leading order in Λ_{QCD}/m_b, in the QCDF approach by using a partonic language and one has [16, 17, 18, 19, 20, 21]:

$$\langle PV|O_i(\mu)|B\rangle = F_j^{B\to P}(m_V^2)\int_0^1 dx T_{ij}^I(x)\phi_V(x) + A_k^{B\to V}(m_P^2)\int_0^1 dy T_{ik}^I(y)\phi_p(y) + \int_0^1 d\xi\int_0^1 dx\int_0^1 dy T_i^{II}(\xi,x,y)\phi_B(\xi)\phi_V(x)\phi_P(y)\ , \quad (8)$$

where ϕ_M (with $M = V,P,B$) are the leading twist light cone distribution amplitudes (LCDA) of valence quark Fock states. The light cone momentum fractions of the constituent quarks of the vector, pseudo-scalar and B mesons are given respectively by x,y, and ξ. The form factors for $B\to P$ and $B\to V$ semi-leptonic decays evaluated at $k^2=0$ are denoted by $F_j^{B\to P}(m_V^2)$ and $A_k^{B\to V}(m_P^2)$. Eq. (8) can be understood via Fig. 2 where a graphical representation of the factorization formula is given. The hadronic

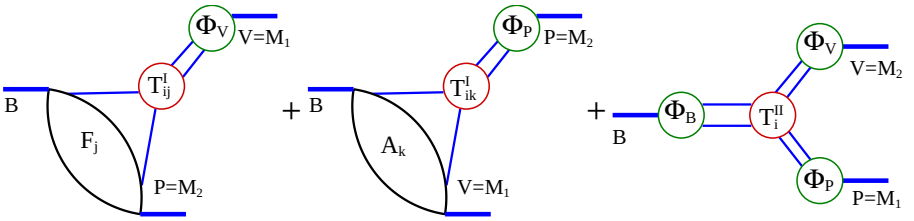

FIGURE 2. Graphical representation of the QCD factorization formula.

decay amplitude involves both soft and hard contributions. At leading order, all the non-perturbative effects are contained in the form factors and the light cone distributions amplitudes. Then, non-factorizable interactions are dominated by hard gluon exchanges (in the case where the $O(\Lambda_{QCD}/m_b)$ terms are neglected) and can be calculated perturbatively, in order to correct the naive factorization approximation. These hard scattering kernels [16, 17, 18, 19, 20, 21, 22], T_{ik}^I and T_i^{II}, are calculable order by order in perturbation theory. The naive factorization terms are recovered by the leading terms of T_{ik}^I coming from the tree level contributions, whereas vertex corrections and penguin corrections are included at higher orders of α_s in T_{ik}^I. The hard interactions (at order $O(\alpha_s)$) between the spectator quark and the emitted meson, at large gluon momentum, are taken into account by T_i^{II}.

2.1. The QCD coefficients a_i

The coefficients a_i [23, 24], have been calculated at next-to-leading order. They contain all the non-factorizable effects at order in α_s. In order to clearly separate every

contribution, the coefficients a_i are written as the sum of,

$$a_i = a_{i,I} + a_{i,II} \,, \tag{9}$$

where the first term includes the naive factorization, the vertex and penguin corrections, while the second term contains the hard spectator interactions. According to the final states, the terms a_i have to be expressed for two different cases: case A corresponds to the situation where the recoiling meson M_1 is a vector and the emitted meson M_2 is a pseudoscalar, and vice-versa for case B. For case A, the coefficients a_i take the form [23, 24],

$$\begin{aligned}
a_{1,I} &= C_1 + \frac{C_2}{N_c^{eff}}\left[1+\frac{C_F\alpha_s}{4\pi}V_M\right], & a_{1,II} &= \frac{\pi C_F\alpha_s}{N_c^{eff2}}C_2 H(BM_1,M_2)\,,\\
a_{2,I} &= C_2 + \frac{C_1}{N_c^{eff}}\left[1+\frac{C_F\alpha_s}{4\pi}V_M\right], & a_{2,II} &= \frac{\pi C_F\alpha_s}{N_c^{eff2}}C_1 H(BM_1,M_2)\,,\\
a_{3,I} &= C_3 + \frac{C_4}{N_c^{eff}}\left[1+\frac{C_F\alpha_s}{4\pi}V_M\right], & a_{3,II} &= \frac{\pi C_F\alpha_s}{N_c^{eff2}}C_4 H(BM_1,M_2)\,,\\
a^p_{4,I} &= C_4 + \frac{C_3}{N_c^{eff}}\left[1+\frac{C_F\alpha_s}{4\pi}V_M\right] + a^p_{4,I,b}\,, & a_{4,II} &= \frac{\pi C_F\alpha_s}{N_c^{eff2}}C_3 H(BM_1,M_2)\,,\\
a_{5,I} &= C_5 + \frac{C_6}{N_c^{eff}}\left[1-\frac{C_F\alpha_s}{4\pi}V'_M\right], & -a_{5,II} &= \frac{\pi C_F\alpha_s}{N_c^{eff2}}C_6 H'(BM_1,M_2)\,,\\
a^p_{6,I} &= C_6 + \frac{C_5}{N_c^{eff}}\left[1-6\frac{C_F\alpha_s}{4\pi}\right] + a^p_{6,I,b}\,, & a_{6,II} &= 0\,,\\
a_{7,I} &= C_7 + \frac{C_8}{N_c^{eff}}\left[1-\frac{C_F\alpha_s}{4\pi}V'_M\right], & -a_{7,II} &= \frac{\pi C_F\alpha_s}{N_c^{eff2}}C_8 H'(BM_1,M_2)\,,\\
a^p_{8,I} &= C_8 + \frac{C_7}{N_c^{eff}}\left[1-6\frac{C_F\alpha_s}{4\pi}\right] + a^p_{8,I,b}\,, & a_{8,II} &= 0\,,\\
a_{9,I} &= C_9 + \frac{C_{10}}{N_c^{eff}}\left[1+\frac{C_F\alpha_s}{4\pi}V_M\right], & a_{9,II} &= \frac{\pi C_F\alpha_s}{N_c^{eff2}}C_{10} H(BM_1,M_2)\,,\\
a^p_{10,I} &= C_{10} + \frac{C_9}{N_c^{eff}}\left[1+\frac{C_F\alpha_s}{4\pi}V_M\right] + a^p_{10,I,b}\,, & a_{10,II} &= \frac{\pi C_F\alpha_s}{N_c^{eff2}}C_9 H(BM_1,M_2)\,,
\end{aligned} \tag{10}$$

where the terms $a^p_{4,I,b}, a^p_{6,I,b}, a^p_{8,I,b}$ and $a^p_{10,I,b}$ are,

$$\begin{aligned}
a^p_{4,I,b} &= \frac{C_F\alpha_s}{4\pi}\frac{P^p_{M,2}}{N_c^{eff}}\,, & a^p_{6,I,b} &= \frac{C_F\alpha_s}{4\pi}\frac{P^p_{M,3}}{N_c^{eff}}\,,\\
a^p_{8,I,b} &= \frac{\alpha}{9\pi}\frac{P^{p,ew}_{M,3}}{N_c^{eff}}\,, & a^p_{10,I,b} &= \frac{\alpha}{9\pi}\frac{P^{p,ew}_{M,2}}{N_c^{eff}}\,.
\end{aligned} \tag{11}$$

In Eqs. (10) and (11) V_M, V'_M represent the vertex corrections, H, H' describe hard gluon exchanges between the spectator quark in the B meson and the emitted meson

(pseudoscalar or vector). $P^{p}_{M,2}, P^{p}_{M,3}, P^{p,ew}_{M,3}, P^{p,ew}_{M,2}$ are the QCD penguin contributions and electroweak penguin contributions, respectively. These quantities are a result of the convolution of hard scattering kernels G, with meson distribution amplitudes, Φ. We refer the reader to Refs. [16, 17, 18, 19, 20, 21] for more details. Other parameters are $C_i \equiv C_i(\mu)$ (in NDR), $\alpha_s \equiv \alpha_s(\mu)$ (next to leading order), and $C_F = (N_c^2 - 1)/2N_c$ with $N_c = 3$.

3. NUMERICAL RESULTS

Assuming that all of the parameters involved in QCD factorization are constrained by independent studies where the input parameters related to factorization were fitted, we concentrate our efforts on the form factor $F_1^{B\to\pi}$ depending on the CKM matrix parameters ρ and η. In order to reach this aim, we have calculated the branching ratios for B decays such as $B^{\pm} \to \rho^0\pi^{\pm}, B^0 \to \rho^{\pm}\pi^0, B^0 \to \rho^{\pm}\pi^{\mp}, B^0 \to \rho^0\pi^0$ and $B^{\pm} \to \omega\pi^{\pm}$ where the annihilation and $\rho - \omega$ mixing contributions were taken into account. All the results are shown in Figs. 3, 4 and 5, and the branching ratios are plotted as a function of the form factor $F_1^{B\to\pi}$ and as a function of the values of ρ and η as well.

By taking into account experimental data from CLEO [25, 26, 27, 28, 29, 30], BELLE [31, 32, 33, 34, 35, 36, 37, 38, 39] and BABAR [40, 41, 42, 43, 44, 45, 46, 47], and comparing theoretical predictions with experimental results, we expect to obtain a constraint on the form factor $F_1^{B\to\pi}$ depending on the CKM matrix element parameters ρ and η. Because of the accuracy of the data, we shall mainly use the CLEO and BELLE data for our analysis rather than those from BABAR. We expect that our results should depend more on uncertainties coming from the experimental data than those from the factorization approach (as opposed to naive factorization) applied to calculate hadronic matrix element $\langle\rho\pi|J_\mu|B\rangle$ since in B decays, $1/m_b$ corrections are very small.

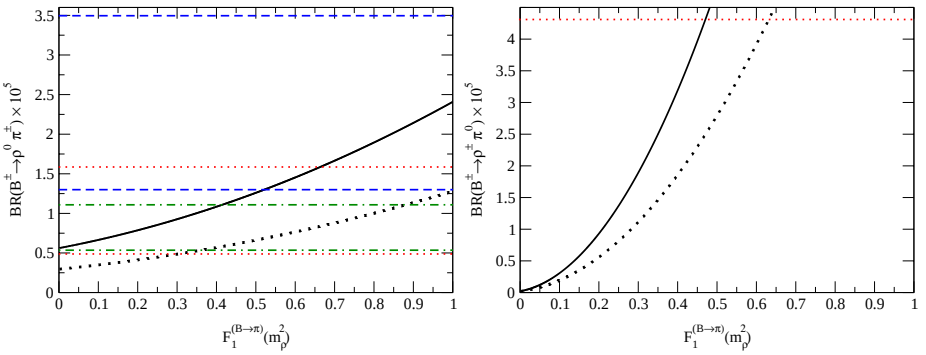

FIGURE 3. Branching ratio for $B^{\pm} \to \rho^0\pi^{\pm}$, for limiting values of the CKM matrix elements (Left hand-side). Branching ratio for $B^{\pm} \to \rho^{\pm}\pi^0$, for limiting values of the CKM matrix elements (Right hand-side). Solid line (dotted line) for max (min) CKM matrix elements. Notation: horizontal dotted lines: CLEO data; horizontal dashed lines: BABAR data; horizontal dot-dashed lines: BELLE data.

For the branching ratio $B^{\pm} \to \rho^0\pi^{\pm}$ (Fig. 3), we found total consistency between the theoretical results and experimental data from CLEO and BELLE. However, these

results allow us to determine an upper limit (between 0.40 and 0.65) for the value of the form factor $F_1^{B\to\pi}$. The weak dependence of the branching ratio on the form factor, $F_1^{B\to\pi}$, is related to the tree and penguin amplitudes which are mainly governed by the form factor $A_0^{B\to\rho}$ rather than $F_1^{B\to\pi}$. Therefore, this branching ratio cannot be used as an efficient way to constrain the form factor $F_1^{B\to\pi}$. Note also that the comparison with BABAR data shows agreement between theory and experiment when $F_1^{B\to\pi}$ is bigger than 0.5.

For the branching ratio $B^{\pm}\to\rho^{\pm}\pi^0$ (Fig. 3), CLEO gives only an upper limit for the branching ratio whereas BABAR and BELLE do not. Based on this upper limit, the value of the form factor $F_1^{B\to\pi}$ must be lower than 0.62. We emphasize that this branching ratio is strongly dependent on the form factor $F_1^{B\to\pi}$ and hence provides an efficient constraint for the value of $F_1^{B\to\pi}$. For the branching ratio $B^0\to\rho^{\pm}\pi^{\mp}$ (shown in Fig. 4), BELLE, BABAR and CLEO give consistent experimental data. The decay amplitude related to this branching ratio is proportional to the form factor $F_1^{B\to\pi}$ and thus allows us to constrain the form factor effectively. Requiring agreement between experimental values and theoretical results yields a central value for $F_1^{B\to\pi}$ which is about 0.3. Note that for these three branching ratios their dependence on the CKM matrix elements ρ and η is strong. Hence we expect to be able to determine limits for their values when more B decay channels are taken into account.

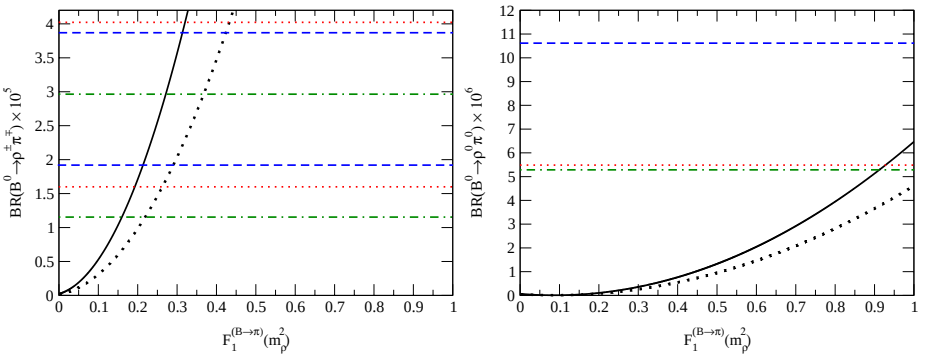

FIGURE 4. Branching ratio for $B^0\to\rho^{\pm}\pi^{\mp}$, for limiting values of the CKM matrix elements (Left hand-side). Branching ratio for $B^0\to\rho^0\pi^0$, for limiting values of the CKM matrix elements (Right hand-side). Solid line (dotted line) for max (min) CKM matrix elements. Notation: horizontal dotted lines: CLEO data; horizontal dashed lines: BABAR data; horizontal dot-dashed lines: BELLE data.

For the branching ratio $B^0\to\rho^0\pi^0$ (Fig. 4), BABAR, BELLE and CLEO only give an upper limit for the branching ratio. However, the branching ratio does not appear to be very sensitive to the CKM matrix elements ρ and η. That could help us to obtain an upper limit for $F_1^{B\to\pi}$ which is not sensitive to ρ and η. We therefore need new data to go further in this case. Finally, we focus on the branching ratio $B^{\pm}\to\omega\pi^{\pm}$, plotted in Fig. 5. There is no agreement with the CLEO data for values of the form factor $F_1^{B\to\pi}$ lower than 0.25 whereas there is a good agreement with BABAR and BELLE for any value of $F_1^{B\to\pi}$. Note that in this case the sensitivity of the branching ratio to the CKM matrix elements is bigger than that to the form factor $F_1^{B\to\pi}$ and does not allow us to

draw any conclusions regarding the value of $F_1^{B\to\pi}$.

To remove systematic errors in branching ratio data given by the B factories, we can look at the ratio R_π of the two following branching ratios: $\mathscr{B}(B^0 \to \rho^\pm \pi^\mp)$ and $\mathscr{B}(B^\pm \to \rho^0 \pi^\pm)$. In Fig. 5 we show the ratio, R_π, as a function of the form factor $F_1^{B\to\pi}$. All the B factory data are in good agreement with theoretical predictions. The results indicate that the ratio is not sensitive to the CKM matrix elements ρ and η whereas it is very sensitive to the value of $F_1^{B\to\pi}$. Comparison with the data shows that $F_1^{B\to\pi}$ is between 0.13 and 0.30 (BELLE), 0.05 and 0.20 (BABAR), and 0.10 and 0.35 (CLEO), respectively. Assuming that the value of $F_1^{B\to\pi}$ at $k^2 = m_\rho^2$ is around 0.30, we have $\mathscr{B}(B^0 \to \rho^\pm \pi^0) \approx 14.2 \times 10^{-6}$ and $\mathscr{B}(B^0 \to \rho^0 \pi^0) < 1 \times 10^{-6}$.

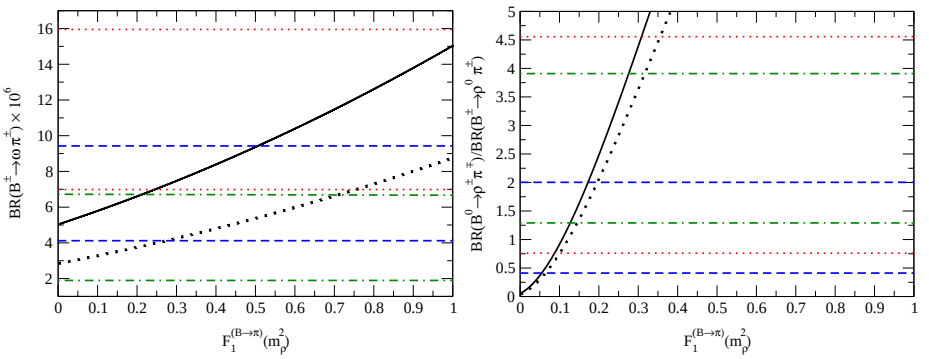

FIGURE 5. Branching ratio for $B^\pm \to \omega\pi^\pm$, for limiting values of the CKM matrix elements (Left hand-side) . The ratio of two $\rho\pi$ branching ratios limiting values of the CKM matrix elements (Right hand-side). Solid line (dotted line) for max (min) CKM matrix elements. Notation: horizontal dotted lines: CLEO data; horizontal dashed lines: BABAR data; horizontal dot-dashed lines: BELLE data.

It has to be pointed out that the annihilation contributions in B decays play an important role since they contribute significantly to the magnitude of the amplitude. The annihilation diagram contribution to the total decay amplitude strongly modifies (in a positive or negative way) the branching ratio $B^- \to \rho^0\pi^-$ according to the value chosen for the phase ϕ_A. This contribution could be bigger than that of $\rho - \omega$ mixing but carries more uncertainties because of its endpoint divergence. We emphasise that these two contributions ($\rho - \omega$ mixing effects and annihilation contributions) are not just simple corrections to the total amplitude, but are important in obtaining a correct description of B decay amplitude.

4. FORM FACTOR $F_1^{B\to\pi}$

Form factors play a major role in the factorization method (naive or QCDF) since they represent the transition between two hadronic states. Their computation is non trivial and may carry large uncertainties, depending on models being used. These models include, say, QCD sum rules, heavy quark effective theory, lattice QCD and light cone QCD. With the available experimental data for the branching ratios, it is now possible for us to constrain $F_1^{B\to\pi}$ in a model-independent way in QCDF.

It has to be noticed that the branching ratios depend on both $F_1^{B\to\pi}$ and N_c^{eff}. In Fig. 6 we show the results regarding the form factor $F_1^{B\to\pi}(m_\rho^2)$ as a function of N_c^{eff}, where we require that all the branching ratios for B decaying into $\rho\pi$ and $\omega\pi$ be consistent with the experimental data provided by CLEO and BELLE. We have excluded the data from BABAR since they are currently not numerous and accurate enough. We have included uncertainties from the CKM matrix element parameters ρ ($0.190 < \rho < 0.268$) and η ($0.284 < \eta < 0.366$) and we have applied the QCD factorization method where all of the final state interaction corrections arising at order α_s are incorporated. We emphasize that the results are model independent.

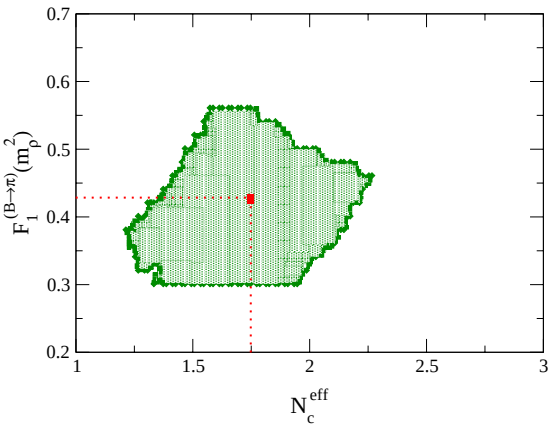

FIGURE 6. $F_1^{B\to\pi}$ as a function of N_c^{eff}. Plot obtained by comparing theoretical results from QCFD with experimental data from BELLE and CLEO for the branching ratios $B\to\rho\pi$ and $B\to\omega\pi$. The plot includes the uncertainties from the CKM matrix element parameters ρ and η.

We found a large common region between BELLE and CLEO for the B decay into $\rho\pi$. From our analysis, $F_1^{B\to\pi}(m_\rho^2)$ varies between 0.3 and 0.57 and N_c^{eff} can take values from 1.25 to 2.25. Their central values are $F_1^{B\to\pi}(m_\rho^2) = 0.43$ and $N_c^{eff} = 1.75$. The result obtained for the form factor $F_1^{B\to\pi}(m_\rho^2)$ reduces one of the main uncertainties in the factorization process. That obtained for the effective number of colours, N_c^{eff}, confirms previous analysis where naive factorization was applied for the same decays [11].

It is well known that the CKM matrix element parameters ρ and η are the main "key" to CP violation within the Standard Model. Recall that the weak phase is mainly governed by the parameter η that provides the imaginary part which is absolutely necessary to obtain an asymmetry between matter and antimatter. Based on our analysis, we are not able to efficiently constrain the CKM matrix parameters ρ and η from the branching ratios for $B\to\rho\pi$. In fact, the common region allowed by CLEO and BELLE data for branching ratios for $B\to\rho\pi$ does not constrain the parameters ρ and η. In the analysis we used the values $0.190 < \rho < 0.268$ and $0.284 < \eta < 0.366$ [48, 49], to which the common region corresponds. However, we can try (as an example) to get some constraints on ρ and η by only taking into account the central values for the form factor $F_1^{B\to\pi}(m_\rho^2)$ and for the effective number of colours N_c^{eff}. According to our work, we find the following limits: $0.205 < \rho < 0.251$ and $0.300 < \eta < 0.351$.

5. CONCLUSION

The calculation of the hadronic matrix elements that appear in the B decay amplitude is non trivial. The main difficulty is to express the hadronic matrix elements which represent the transition between the meson B and the final state.

We have investigated the branching ratios for $B \to \rho\pi, B \to \omega\pi$ within the QCDF approach. Comparisons were made with experimental results from BABAR, BELLE and CLEO. Based on our analysis of branching ratios in B decays, we have constrained the form factor, $F_1^{B\to\pi}(m_\rho^2)$, and the effective number of colours, N_c^{eff}. More accurate experimental data regarding branching ratios in B decays will provide more accurate results, which will be helpful in gaining further knowledge of direct CP violation in B decays.

This work could be extended to more B decays. It would be very interesting to constrain our parameters by investigating channels other than $\rho\pi$ for branching ratios and asymmetries. By including more channels, we will use more experimental data and hence be able to obtain better results for our parameters. In the QCD factorization framework, annihilation contributions could be subject to discussions. Clarifying this point would be very helpful in obtaining more accurate theoretical predictions. For example, it is important to solve the problem related to the end point integral divergence [16] which is parameterized without any strong physical motivation. Moreover, the annihilation contributions have not been included within the QCDF method. To obtain a consistent framework, it would be better to find a way to include them within QCDF.

Acknowledgements
This work was supported in part by the Australian Research Council and the University of Adelaide.

REFERENCES

1. Buras, Andrzej J., Lect. Notes Phys. **558** (2000) 65.
2. Buras, Andrzej J., hep-ph/9806471.
3. Buchalla, Gerhard and Buras, Andrzej J. and Lautenbacher, Markus E., Rev. Mod. Phys. **68** (1996) 1125.
4. Stech, Berthold, hep-ph/9706384.
5. Buras, Andrzej J., Nucl. Instrum. Meth. **A368** (1995) 1.
6. Fakirov, Dotcho and Stech, Berthold, Nucl. Phys. **B133** (1978) 315.
7. Cabibbo, N. and Maiani, L., Phys. Lett. **B73** (1978) 418.
8. Dugan, Michael J. and Grinstein, Benjamin, Phys. Lett. **B255** (1991) 583.
9. Bjorken, James D., Nucl. Phys. Proc. Suppl. **11** (1989) 325.
10. O. Leitner, X.-H. Guo and A.W. Thomas, Phys. Rev. **D66** (2002) 096008.
11. X.-H. Guo, O. Leitner and A.W. Thomas, Phys. Rev. **D63** (2001) 056012.
12. Z.J. Ajaltouni, O. Leitner, P. Perret, C. Rimbault and A.W. Thomas, Eur. Phys. J. **C29** (2003), 215-233.
13. Quinn, Helen R., hep-ph/9912325.
14. Cheng, Hai-Yang, Phys. Lett. **B335** (1994) 428.
15. Cheng, Hai-Yang, Phys. Lett. **B395** (1997) 345.

16. Beneke, M. and Buchalla, G. and Neubert, M. and Sachrajda, Christopher T., Phys. Rev. Lett. **83** (1999) 1914.
17. Neubert, Matthias, AIP Conf. Proc. **602** (2001) 168.
18. Neubert, Matthias, Nucl. Phys. Proc. Suppl. **99B** (2001) 113.
19. Beneke, M. J., Phys. **G27** (2001) 1069.
20. Beneke, M., hep-ph/0207228.
21. Beneke, M., hep-ph/9910505.
22. Beneke, M. and Buchalla, G. and Neubert, M. and Sachrajda, Christopher T., hep-ph/0007256.
23. Beneke, M. and Buchalla, G. and Neubert, M. and Sachrajda, Christopher T., Nucl. Phys. **B606** (2001) 245.
24. Beneke, M. and Buchalla, G. and Neubert, M. and Sachrajda, Christopher T., Nucl. Phys. **B591** (2000) 313.
25. Gao, Yongsheng and Wurthwein, Frank, CLEO collaboration, hep-ex/9904008.
26. Jessop, C. P. and others, CLEO collaboration, Phys. Rev. Lett. **85** (2000) 2881.
27. Schwarthoff, H., CLEO collaboration, hep-ex/0205015.
28. De Monchenault, Gautier Hamel, hep-ex/0305055.
29. Briere, Roy A., CLEO collaboration, AIP Conf. Proc. **618** (2002) 159.
30. Zhao, Xin, hep-ex/0101013.
31. Abe, K. and others, BELLE collaboration, hep-ex/0107051.
32. Bozek, A., BELLE collaboration, hep-ex/0104041.
33. Lu, R. S. and others, BELLE collaboration, Phys. Rev. Lett. **89** (2002) 191801.
34. Casey, B. C. K. and others, BELLE collaboration, Phys. Rev. **D66** (2002) 092002.
35. Abe, K. and others, BELLE collaboration, Phys. Rev. **D65** (2002) 092005.
36. Garmash, Alexei, BELLE collaboration, hep-ex/0207003.
37. Gordon, A. and others, BELLE collaboration, Phys. Lett. **B542** (2002) 183.
38. Iijima, Toru, BELLE collaboration, hep-ex/0105005.
39. Kinoshita, Kay, BELLE collaboration, Nucl. Instrum. Meth. **A462** (2001) 77.
40. Aubert, B. and others, BABAR collaboration, Phys. Rev. Lett. **87** (2001) 221802.
41. Aubert, B. and others, BABAR collaboration, hep-ex/0206004.
42. Olsen, J., BABAR collaboration, Int. J. Mod. Phys. **A16S1A** (2001) 468.
43. Aubert, B. and others, BABAR collaboration, hep-ex/0008058.
44. Schietinger, Thomas, BABAR collaboration, hep-ex/0105019.
45. Sciolla, G., BABAR collaboration, Nucl. Phys. Proc. Suppl. **99B** (2001) 135.
46. Cavoto, Gianluca, BABAR collaboration, hep-ex/0105018.
47. Aubert, B. and others, BABAR collaboration, Phys. Rev. Lett. **87** (2001) 151802.
48. Abbaneo, D. and others, hep-ex/0112028.
49. Groom, D. E. and others, Eur. Phys. J. **C15** (2000) 1.